RESEARCH ARTICLE

Simulation of the typical Poisson-Voronoi-Cox-Voronoi cell

FRANK FLEISCHER†, CATHERINE GLOAGUEN‡, VOLKER SCHMIDT§ and
FLORIAN VOSS*§

† Medical Data Services/Biostatistics
Boehringer-Ingelheim Pharma GmbH & Co. KG, D-88397 Biberach, Germany
E-mail: frank.fleischer@boehringer-ingelheim.com
Phone: +49 7351 542372
Fax: +49 7351 545986

‡ France Telecom Research & Development
F-92131 Issy les Moulineaux Cedex 9, France
E-mail: catherine.gloaguen@orange-ftgroup.com
Phone: +33 1 45 29 64 41
Fax: +33 1 45 29 63 07

§ Institute of Stochastics
Ulm University, D-89069 Ulm, Germany
E-mail: volker.schmidt@uni-ulm.de, florian.voss@uni-ulm.de
Phone: +49 731 5023531
Fax: +49 731 5023649

(*April 1, 2008*)

We consider stationary Poisson-Voronoi tessellations (PVT) in the Euclidean plane and study properties of Voronoi tessellations induced by linear Poisson processes on the edges of the PVT. We are especially interested in simulation algorithms for the typical cell. Two different simulation algorithms are introduced. The first algorithm directly simulates the typical cell whereas the second algorithm simulates cells from which distributional properties of the typical cell can be obtained. This second algorithm can also be used for simulating the typical cell of other Cox-Voronoi tessellations. The implementation of both algorithms is tested for their correctness using random software tests. Then different cell characteristics are studied by simulation and compared to the typical cell of Poisson-Voronoi tessellations and Cox-Voronoi tessellations based on linear Poisson processes on the lines of Poisson line processes. Our results can be applied for example in the analysis of telecommunication networks and vesicle paths on cytoskeletal networks.

Acknowledgement

1.   Introduction

Voronoi tessellations are one of the most important models for subdividing the Euclidean plane into convex and compact polygons. To each point of a set of points called nuclei a polygon is constructed according to the nearest neighbour principle. These polygons are then called the cells of the Voronoi tessellation. Voronoi tessellations are widely applied in many different fields, e.g. economics, biology and telecommunication; see [14] and references therein. Important classes of random tessellations are Voronoi tessellations constructed from the realizations of stationary point processes. Examples are Poisson-Voronoi tessellations (PVT) and Cox-Voronoi tessellations, where the generating point processes are homogeneous Poisson processes and Cox-processes, respectively; see [2], [4], [5], [14], [18].

Interesting models for applications are points processes which are located on the lines and curves of planar line and fibre processes, respectively. In the field of telecommunication the lines and curves can represent roads and the points locations of telecommunication equipment ([7]), whereas in life sciences, e.g., the lines can represent blood arteries or filament structures in biological tissues or cells and the points locations of vesicles ([17]).

In this paper, we consider Voronoi tessellations whose nuclei are placed as linear Poisson processes on the edges of PVT. We call this type of tessellations Poisson-Voronoi-Cox-Voronoi tessellations (PVCVT) since the nuclei form a Cox process. In the context of telecommunication networks the cells of PVCVT can be considered e.g. as serving zones of network components located at the nuclei.

Many interesting characteristics of a stationary tessellation can be calculated by characteristics of its typical cell ([18]). The typical cell can be regarded as the cell chosen purely at random out of all possible cells of the tessellation. For stationary and ergodic Voronoi tessellations the typical cell can be thought of as the cell whose nucleus is located at the origin under the condition that the generating point process has a point at the origin. In the following, we derive two algorithms to simulate the typical cell of PVCVT. One algorithm simulates the typical cell directly whereas the other algorithm simulates a (random) cell from which distributional properties of the typical cell can be obtained by a subsequent weighting.

Naturally, the implementation of these two algorithms have to be tested for correctness. Since the output is random, tests for randomized software can be applied, see [3], [5], [10]. An advantage of having two different algorithms is that we can use them to compare their outputs and hence test the outputs against each other. Note that all these software tests are based on statistical significance tests.

We use the algorithms to compute first-order and second-order moments of several cell characteristics like the number of vertices, the perimeter and the area of the typical cell of PVCVT. Since analytical formulae for such characteristics are unknown simulation studies are useful to get information about their distributional properties.

As we have two algorithms it is of interest to determine which algorithm is preferable. Thus we compare the two algorithms with respect to runtime and precision. Clearly an algorithm with short runtime is desired. On the other hand, since the output of the algorithms is random, it is desired to have an algorithm with low variances in the output to get more precise results from the simulations.

Finally, we compare the results of our simulations for the typical cell of PVCVT to the results for the typical cell of PVT and Poisson-Line-Cox-Voronoi tessellations (PLCVT). The comparison with previous simulation studies for the PLCVT ([5]) is especially interesting, since both can represent possible models for telecom-

munication networks ([6]).

The paper is organized as follows. First we introduce the PVCVT model and some mathematical background in Section 2. In Section 3, our simulation algorithms are derived and explained in detail. Then, in Section 4, we present numerical results. First we discuss methods for testing and validating the implementation of these algorithms and we compare the precision of the two algorithms. Then we estimate distributional properties of the typical cell of PVCVT and compare them to results for other tessellation models like PVT and PLCVT.

2. Poisson-Voronoi-Cox-Voronoi tessellations

In this section, we introduce the basic notation and mathematical background used in this paper. For more details about point processes and random tessellations see for example [14], [16] and [18].

2.1. *Point processes and random tessellations*

In the following, by $\mathbb{R}^2$ and $\mathbb{N}$ we denote the Euclidean plane and the set of non–negative integers, respectively.

Point processes. Let $\mathcal{B}(\mathbb{R}^2)$ denote the family of Borel sets of $\mathbb{R}^2$. Denote the Lebesgue measure on $\mathcal{B}(\mathbb{R}^2)$ by ν_2 and define the translation $B + x$ for sets $B \subset \mathbb{R}^2$ and $x \in \mathbb{R}^2$ by $B + x = \{y + x : y \in B\}$. We use the notation N for the family of all simple and locally finite counting measures φ on $\mathcal{B}(\mathbb{R}^2)$, where each $\varphi \in N$ can be expressed by the (countable) sum $\varphi = \sum_{i=1}^{n} \delta_{x_i}$ for $n \in \mathbb{N} \cup \{\infty\}$. Here, δ_x with $\delta_x(B) = \mathbb{1}_B(x)$ is the Dirac measure on $\mathcal{B}(\mathbb{R}^2)$. In the context of counting measures we call $x \in \mathbb{R}^2$ an atom of φ if $\varphi(\{x\}) > 0$. Sometimes we identify φ with its atoms and write $\varphi = \{x_n\}_{n \geq 1}$. We equip N with the σ–algebra $\mathcal{N}$ generated by all sets of the form $\{\varphi \in N : \varphi(B) = j\}$ with $j \in \mathbb{N}$ and bounded $B \in \mathcal{B}(\mathbb{R}^2)$. Moreover, by $t_x : N \to N$ we denote the shift operator defined by $t_x\varphi(B) = \varphi(B + x)$ for all $x \in \mathbb{R}^2$ and $\varphi \in N$.

A measurable mapping $X : \Omega \to N$ from some probability space $(\Omega, \mathcal{A}, \mathbb{P})$ into the measurable space $(N, \mathcal{N})$ is called a *random point process* in $\mathbb{R}^2$. There are different ways of looking at point processes. One possibility is to regard them as random counting measures. Then $X(B)$ can be interpreted as the (random) number of atoms of X in $B \in \mathcal{B}(\mathbb{R}^2)$. Another possibility is to identify a point process X with the random set $\{X_n\}_{n \geq 1}$ of its atoms and then use the notation $X = \{X_n\}_{n \geq 1}$.

The probability measure $\mathbb{P}_X$ defined on $\mathcal{N}$ by $\mathbb{P}_X(A) = \mathbb{P}(X \in A)$ for $A \in \mathcal{N}$ is called the distribution of X. A point process X is called stationary if X and $t_x X$ have the same distribution for any $x \in \mathbb{R}^2$.

We define the *intensity measure* $\mu : \mathcal{B}(\mathbb{R}^2) \to [0, \infty]$ of a point process X by

$$\mu(B) = \mathbb{E}X(B), \qquad B \in \mathcal{B}(\mathbb{R}^2). \tag{1}$$

For stationary X there exists a constant $\lambda \geq 0$ such that $\mu(B) = \lambda\nu_2(B)$ for each $B \in \mathcal{B}(\mathbb{R}^2)$, where λ is called the *intensity* of the point process X.

The point process X is called a *Poisson process* if

$$\mathbb{P}(X(B) = k) = e^{-\mu(B)} \frac{\mu(B)^k}{k!}, \qquad B \in \mathcal{B}(\mathbb{R}^2), k \in \mathbb{N} \tag{2}$$

for some (locally finite and diffuse) measure $\mu : \mathcal{B}(\mathbb{R}^2) \to [0, \infty]$.

Random measures. Locally finite counting measures are a special case of locally finite measures on $\mathcal{B}(\mathbb{R}^2)$. We denote the set of all locally finite measures on $\mathcal{B}(\mathbb{R}^2)$ by M. Let $\mathcal{M}$ denote the smallest σ–algebra such that the mappings $\eta \longmapsto \eta(B)$ are measurable for all $\eta \in M$ and bounded $B \in \mathcal{B}(\mathbb{R}^2)$. Furthermore, we define the shift operator $t_x : M \to M$ in the same way as for counting measures.

We call a measurable mapping $\Lambda : \Omega \to M$ from some probability space $(\Omega, \mathcal{A}, \mathbb{P})$ into the measurable space $(M, \mathcal{M})$ a *random measure* on $\mathcal{B}(\mathbb{R}^2)$. In the same way as for point processes we can define the distribution $\mathbb{P}_\Lambda$, stationarity and the intensity of Λ.

Random tessellations as planar marked point processes. A *tessellation* in $\mathbb{R}^2$ is a countable family $\tau = \{\xi_n\}_{n \geq 1}$ of compact and convex polygons fulfilling the conditions int $\xi_n \neq \emptyset$ for all n, int $\xi_n \cap$ int $\xi_m = \emptyset$ for all $n \neq m$, $\bigcup_{n \geq 1} \xi_n = \mathbb{R}^2$, and $\sum_{n \geq 1} \mathbb{I}_{\{\xi_n \cap B \neq \emptyset\}} < \infty$ for any bounded set $B \subset \mathbb{R}^2$. The polygons ξ_n are called the *cells* of the tessellation τ. If $o \in \xi_n$, then ξ_n is called the *zero cell*, where $o \in \mathbb{R}^2$ denotes the origin. Furthermore, we use the notation $\tau^{(1)}$ for the edge set of τ, and $\mathbb{T}$ for the family of all tessellations in $\mathbb{R}^2$. For any compact and convex polygon $\xi \neq \emptyset$ we can define a unique point $\alpha(\xi) \in \xi$ fulfilling $\alpha(\xi + x) = \alpha(\xi) + x$ for all $x \in \mathbb{R}^2$, where we call $\alpha(\xi)$ an *associated point* or *nucleus* of ξ. It can be chosen e.g. as the centre of gravity of ξ. Let $\mathcal{P}^o$ denote the space of all (nonempty) compact and convex polygons in $\mathbb{R}^2$ with associated point at o and let $\mathcal{B}(\mathcal{P}^o)$ denote the Borel–σ–algebra on $\mathcal{P}^o$ with respect to the Hausdorff metric.

Let $N_{\mathcal{P}^o}$ denote the set of all counting measures $\psi : \mathcal{B}(\mathbb{R}^2) \otimes \mathcal{B}(\mathcal{P}^o) \to \mathbb{N} \cup \{\infty\}$ that are simple and locally finite in the first component. Then a σ–algebra $\mathcal{N}_{\mathcal{P}^o}$ on $N_{\mathcal{P}^o}$ can be constructed in the same way as $\mathcal{N}$ on N. A measurable mapping $T : \Omega \to N_{\mathcal{P}^o}$ from some probability space $(\Omega, \mathcal{A}, \mathbb{P})$ into the measurable space $(N_{\mathcal{P}^o}, \mathcal{N}_{\mathcal{P}^o})$ is called a *random marked point process* in $\mathbb{R}^2$ with mark space $(\mathcal{P}^o, \mathcal{B}(\mathcal{P}^o))$. Note that we can identify T with a random set $\{[X_n, \Xi_n^o]\}_{n \geq 1}$, where $\Xi_n^o \in \mathcal{P}^o$ and $X_n \in \mathbb{R}^2$. A marked point process $T = \{[X_n, \Xi_n^o]\}_{n \geq 1}$ is called *stationary* if T and $t_x T$ have the same distribution for any $x \in \mathbb{R}^2$, where $t_x \tau = \{[x_n - x, \xi_n^o]\}_{n \geq 1}$ for any $\tau = \{[x_n, \xi_n^o]\}_{n \geq 1} \in N_{\mathcal{P}^o}$. If $\{\Xi_n\}_{n \geq 1} \in \mathbb{T}$ almost surely, where $\Xi_n = \Xi_n^o + X_n$, then we call T a random tessellation. Thus, a random tessellation consists of the point process $X = \{X_n\}_{n \geq 1}$ of nuclei which are marked with the cells $\{\Xi_n^o\}_{n \geq 1}$ centred at the origin. If T is stationary, then we define the intensity λ_T of the random tessellation T as the intensity of X.

Note that a random tessellation T can also be identified with the random closed set of its edges which is denoted by $T^{(1)}$. For details about random closed sets see e.g. [12].

Voronoi tessellations. For a point process $X = \{X_n\}_{n \geq 1}$ in $\mathbb{R}^2$ we can define the random polygons $\Xi_n = \{x \in \mathbb{R}^2 : |x - X_n| \leq |x - X_m| \forall m \neq n\}$. Note that Ξ_n can be written as the intersection of (countably many) half-planes $H(X_n, X_m) = \{x \in \mathbb{R}^2 : |x - X_n| \leq |x - X_m|\}$, i.e. $\Xi_n = \bigcap_{m \neq n} H(X_n, X_m)$. If $\{\Xi_n\}_{n \geq 1} \in \mathbb{T}$ almost surely, then we call $T_X = \{\Xi_n\}_{n \geq 1}$ the *Voronoi tessellation* induced by X. If the underlying point process X is a Poisson process, then we call the Voronoi tessellation T_X a *Poisson-Voronoi tessellation* (PVT).

2.2. *Poisson-Voronoi-Cox-Voronoi tessellations*

We now introduce the notion of a Poisson-Voronoi-Cox point process X_c. This is a Cox process, or doubly stochastic Poisson process, whose points are located on the edges of a PVT. Let X_p be a stationary Poisson process in $\mathbb{R}^2$ with intensity λ_p, where T_{X_p} denotes the PVT induced by X_p and $T_{X_p}^{(1)}$ the random closed set of the

(a) Poisson-Voronoi-Cox point process (black) and the underlying PVT (grey)

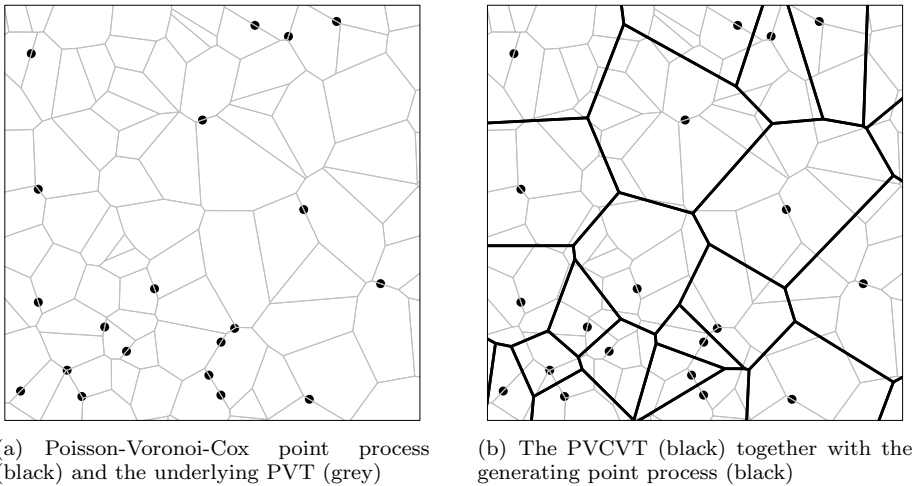(b) The PVCVT (black) together with the generating point process (black)

Figure 1. Realization of a Poisson-Voronoi-Cox point process (left) and the generated PVCVT (right)

edges of T_{X_p}. Then, for a given realization of T_{X_p}, the points of the Cox process X_c are placed on $T_{X_p}^{(1)}$ as linear Poisson processes with linear intensity $\lambda_\ell > 0$. Thus, formally, X_c is a Cox process with random driving measure $\Lambda_{X_c} : \mathcal{B}(\mathbb{R}^2) \to [0, \infty]$ given by

$$\Lambda_{X_c}(B) = \lambda_\ell \nu_1(B \cap T_{X_p}^{(1)}), \qquad B \in \mathcal{B}(\mathbb{R}^2), \tag{3}$$

where ν_1 denotes the 1-dimensional Hausdorff measure on $T_{X_p}^{(1)}$. Thus, X_c is called a *Poisson-Voronoi-Cox process*. In the following, by T_{X_c} we will denote the Voronoi tessellation induced by the Cox process X_c and call it a *Poisson-Voronoi-Cox-Voronoi tessellation* (PVCVT). Realizations of X_c and T_{X_c} are displayed in Figures 1(a) and 1(b), respectively. Notice that X_c is a stationary point process with intensity

$$\lambda_c = 2\lambda_\ell \sqrt{\lambda_p}, \tag{4}$$

since $2\sqrt{\lambda_p} = \mathbb{E}\nu_1([0, 1]^2 \cap T_{X_p}^{(1)})$. Actually, X_c can be fully characterized by the parameters λ_ℓ and λ_p. We also remark that X_c is isotropic and ergodic due to the isotropy and ergodicity of T_{X_p}.

3.   The typical cell of PVCVT

In this section we derive two algorithms that can be used for the estimation of distributional properties of the typical cell of PVCVT. The first algorithm is designed to directly simulate the typical cell, whereas the second algorithm simulates a random polygon from which distributional properties of the typical cell can be obtained by subsequent weighting. The latter algorithm has the advantage that it can be applied to any Cox process concentrated on the edges of a stationary tessellation, whereas the direct algorithm is specifically designed for PVCVT. But first we define Palm probabilities and the notion of the typical cell.

3.1.   *Palm probabilities and the typical cell*

The *Palm distribution* $\mathbb{P}_X^*$ of a stationary point process $X = \{X_n\}_{n \geq 1}$ with intensity λ is a probability distribution on $\mathcal{N}$, which is defined by

$$\mathbb{P}_X^*(A) = \lambda^{-1}\, \mathbb{E}\#\{n \geq 1 : X_n \in [0,1)^2, t_{X_n}X \in A\}, \quad A \in \mathcal{N}. \qquad (5)$$

It can be interpreted as the conditional distribution of X under the condition that one point is located at the origin. In a similar way, considering a stationary tessellation T as a stationary marked point process $\{[X_n, \Xi_n^o]\}_{n \geq 1}$ with intensity λ_T, we define the Palm distribution $\mathbb{P}_T^*$ on $\mathcal{N}_{\mathcal{P}^o} \otimes \mathcal{B}(\mathcal{P}^o)$ by

$$\mathbb{P}_T^*(A \times G) = \lambda_T^{-1}\, \mathbb{E}\#\{n \geq 1 : X_n \in [0,1)^2, \Xi_n^o \in G, t_{X_n}T \in A\} \qquad (6)$$

for any $A \in \mathcal{N}_{\mathcal{P}^o}$ and $G \in \mathcal{B}(\mathcal{P}^o)$, and the *Palm mark distribution* $\mathbb{P}_T^{(o)}$ of T by

$$\mathbb{P}_T^{(o)}(G) = \lambda_T^{-1}\, \mathbb{E}\#\{n \geq 1 : X_n \in [0,1)^2, \Xi_n^o \in G\}, \quad G \in \mathcal{B}(\mathcal{P}^o). \qquad (7)$$

The Palm probability $\mathbb{P}_T^*(A \times G)$ can be interpreted as the conditional probability that T belongs to A under the condition that T has a nucleus at the origin, where the cell of this nucleus belongs to G. A random polygon $\Xi^* : \Omega \to \mathcal{P}^o$ that is distributed according to $\mathbb{P}_T^{(o)}$ is called the *typical cell* of T. It can be regarded as the cell at the origin under the condition that the origin is a nucleus of T. Note that the intensity λ_T of T is related to the expected area of Ξ^* by $\lambda_T^{-1} = \mathbb{E}\nu_2(\Xi^*)$. For Voronoi tessellations T_X the typical cell can be regarded as the cell at the origin if X is distributed according to $\mathbb{P}_X^*$. Furthermore, we can define the *Palm distribution* $\mathbb{P}_\Lambda^*$ of a stationary random measure Λ with intensity $\lambda > 0$ by

$$\mathbb{P}_\Lambda^*(A) = \lambda^{-1}\, \mathbb{E}\left(\int_{[0,1]^2} \mathbb{I}_A(t_x\Lambda)\, \Lambda(dx)\right), \quad A \in \mathcal{M}. \qquad (8)$$

3.2.   *The direct simulation algorithm*

The direct algorithm uses a result recently derived in [1]. First note that the Palm distribution $\mathbb{P}_{X_c}^*$ of a stationary Cox process X_c with random driving measure Λ_{X_c} is given by $\mathbb{P}_{X_c}^* = \delta_{\delta_o} * \mathbb{P}_{\Lambda_{X_c}^*}$, where $\mathbb{P}_{\Lambda_{X_c}^*}$ is the distribution of a Cox process with random driving measure $\Lambda_{X_c}^*$, the conditional version of the driving measure Λ_{X_c} under its Palm distribution $\mathbb{P}_{\Lambda_{X_c}}^*$ (see e.g. [18], p. 156).

In the case of Poisson-Voronoi-Cox processes X_c with linear intensity λ_ℓ, we first show that $\Lambda_{X_c}^*$ can be regarded as the product of the linear intensity λ_ℓ and the 1-dimensional Hausdorff measure ν_1 concentrated on the edge set $\widetilde{T}_{X_p}^{(1)}$ of the Palm version $\widetilde{T}_{X_p}$ of the PVT T_{X_p} seen from the typical point of X_c, i.e., a point chosen at random on the edges of the PVT T_{X_p}.

Lemma 3.1:   *Let Λ_{X_c} be the stationary random measure given in* (3). *Then*

$$\Lambda_{X_c}^*(B) = \lambda_\ell \nu_1(B \cap \widetilde{T}_{X_p}^{(1)}), \qquad B \in \mathcal{B}(\mathbb{R}^2),$$

where $\widetilde{T}_{X_p}^{(1)}$ is distributed according to $\mathbb{P}_{T_{X_p}^{(1)}}^*$, the Palm distribution with respect to the 1-dimensional Hausdorff measure on $T_{X_p}^{(1)}$.
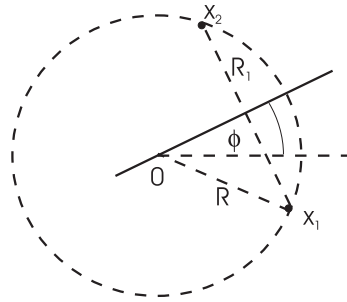
Figure 2. Line segment passing through the origin with the generating points

Proof: For a deterministic tessellation τ we can identify the measure $\eta(\cdot) = \lambda_\ell \nu_1(\cdot \cap \tau^{(1)})$ with τ and write $\eta(\tau)$. Note that $\eta(t_x \tau) = t_x \eta(\tau)$ for all $x \in \mathbb{R}^2$, where t_x is the shift operator introduced in Section 2. Then, by the definition of the Palm distribution $\mathbb{P}^*_{\Lambda_{X_c}}$ given in (8) and using (4), we get that for $A \in \mathcal{M}$

$$
\begin{aligned}
\mathbb{P}^*_{\Lambda_{X_c}}(A) &= \frac{1}{\lambda_c} \int_M \int_{[0,1]^2} \mathbb{I}_A(t_x \eta)\, \eta(dx)\, \mathbb{P}_{\Lambda_{X_c}}(d\eta) \\
&= \frac{1}{2\sqrt{\lambda_p}} \int_{\mathbb{T}} \int_{[0,1]^2 \cap \tau^{(1)}} \mathbb{I}_A(t_x \eta(\tau))\, \nu_1(dx)\, \mathbb{P}_{T_{X_p}}(d\tau) \\
&= \mathbb{P}^*_{T^{(1)}_{X_p}}(\{\tau \in \mathbb{T} : \eta(\tau) \in A\}),
\end{aligned}
$$

where the last equality is obtained from the definition of the Palm distribution $\mathbb{P}^*_{T^{(1)}_{X_p}}$ given in (8). Thus $\eta(\widetilde{T}_{X_p})(\cdot) = \lambda_\ell \nu_1(\cdot \cap \widetilde{T}^{(1)}_{X_p})$ has the same distribution as $\Lambda^*_{X_c}$. $\qquad\square$

In particular, under $\mathbb{P}^*_{\Lambda_{X_c}}$, a line segment of the underlying Voronoi tessellation passes through the origin. Then, it is obvious that those two points X_1 and X_2 with the smallest distance from the origin of the point process $\widetilde{X}_p = \{X_n\}_{n \geq 1}$ which generates this Voronoi tessellation, have to be on a circle around the origin. The positions of these two points can be described by the random variables R, R_1 and Φ. Here, Φ is the angle of the line segment, $R = |X_1|$ is the distance of the points X_1 and X_2 to the origin and $R_1 = |X_1 - X_2|/2$ is half the distance between the points, see Figure 2.

We now state a result which is a special case of Theorem 1.1 in [1]. It will be essentially used in our direct simulation algorithm.

Lemma 3.2: *Under $\mathbb{P}^*_{\Lambda_{X_c}}$ the following holds.*

(i) *The random variables $(\{X_n : |X_n| > R\}, R)$, R_1^2/R^2 and Φ are independent.*
(ii) *R^2 is gamma distributed with shape parameter 1.5 and scale parameter $1/(\lambda_p \pi)$.*
(iii) *The conditional distribution of $\{X_n : |X_n| > R\}$ given $R = r$ is the distribution of a stationary Poisson process in $\mathbb{R}^2 \backslash B(o, r)$ with intensity λ_p.*
(iv) *R_1^2/R^2 is beta distributed with parameters 1 and $1/2$.*
(v) *Φ is uniformly distributed on $[0, 2\pi)$.*

Lemma 3.1 and Lemma 3.2 yield the following simulation algorithm for the typical cell Ξ^*_c of T_{X_c}. We first give an overview of the algorithm, technical details are explained later.

1. Simulate two random variables $R^2 \sim \Gamma(1.5, 1/(\lambda_p \pi))$ and $\tilde{R}^2 \sim B(1, 1/2)$.
2. Construct $X_1 = (\sqrt{R^2 - \tilde{R}^2 R^2}, \tilde{R}R)$ and $X_2 = (\sqrt{R^2 - \tilde{R}^2 R^2}, -\tilde{R}R)$.
3. Simulate a Poisson process $X_{p,R} = \{X_n\}_{n \geq 3}$ radially outside $B(o, R)$ and add X_1 and X_2 to obtain $\widetilde{X}_p = \{X_n\}_{n \geq 1}$.
4. Construct cells of the Voronoi tessellation $\widetilde{T}_{X_p}$ induced by $\widetilde{X}_p$.
5. Simulate points $\{X_{n,c}\}_{n \geq 2}$ on $\widetilde{T}_{X_p}^{(1)}$ according to linear Poisson processes.
6. Add the origin $X_{1,c} = o$ to $\{X_{n,c}\}_{n \geq 2}$ and construct the Voronoi cell around o with respect to $X_c^* = \{X_{n,c}\}_{n \geq 1}$.

In order to get a realization of the typical cell Ξ_c^* we still have to apply an isotropic rotation, but since all characteristics we are considering in this paper are rotation invariant we can in general omit this final rotation step. A sketch of the different steps of the simulation algorithm is shown in Figure 3.
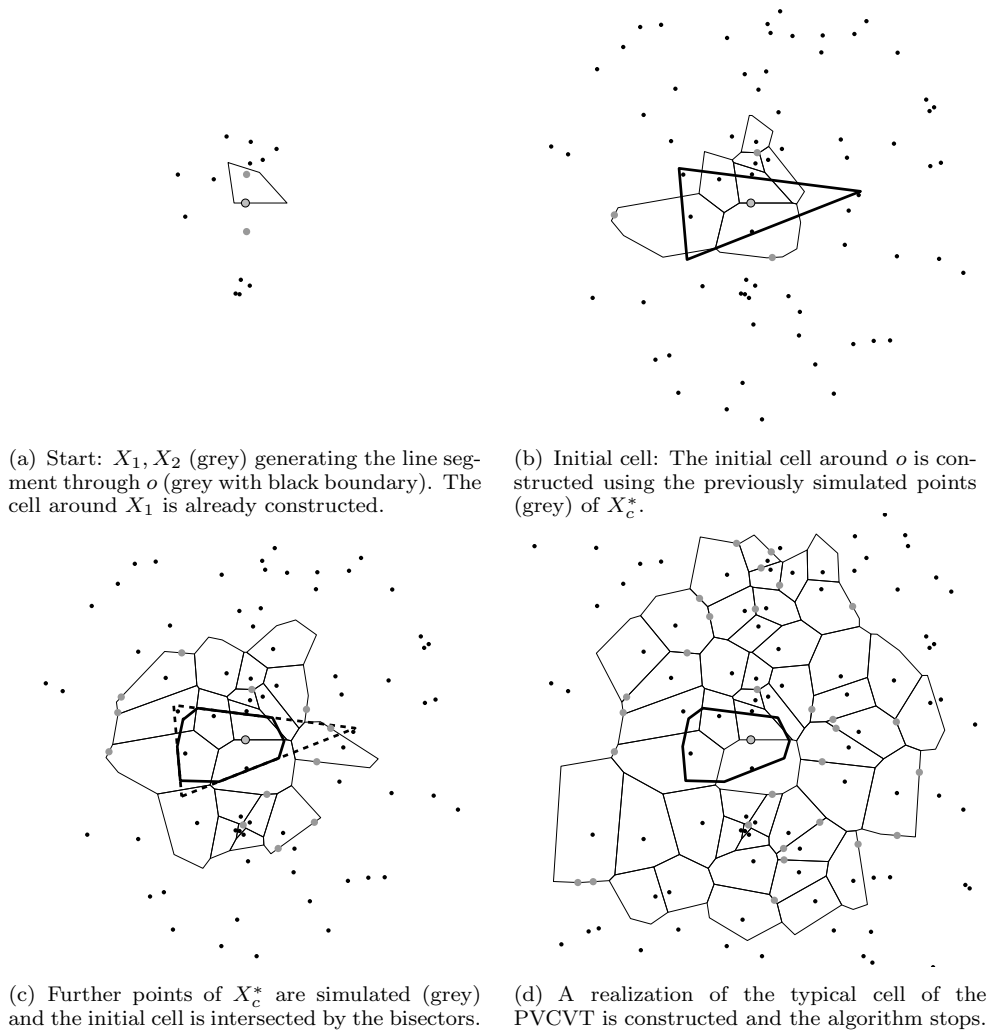

(a) Start: X_1, X_2 (grey) generating the line segment through o (grey with black boundary). The cell around X_1 is already constructed.

(b) Initial cell: The initial cell around o is constructed using the previously simulated points (grey) of X_c^*.

(c) Further points of X_c^* are simulated (grey) and the initial cell is intersected by the bisectors.

(d) A realization of the typical cell of the PVCVT is constructed and the algorithm stops.

Figure 3. Direct simulation of the typical PVCV cell

Of course, some technical details have to be taken into account. The simulation of points of $\widetilde{X}_p$ and construction of cells of $\widetilde{T}_{X_p}$ on the one hand and points of X_c^* on the other hand have to be done in an alternating fashion. First X_1 and X_2 have to be simulated and given $R = |X_1|$ the points of $X_{p,R}$ have to be simulated radially

(a) Stopping criterion: If the circle (grey) is contained in the polygon of the outer vertices (dashed segments) the algorithm stops.

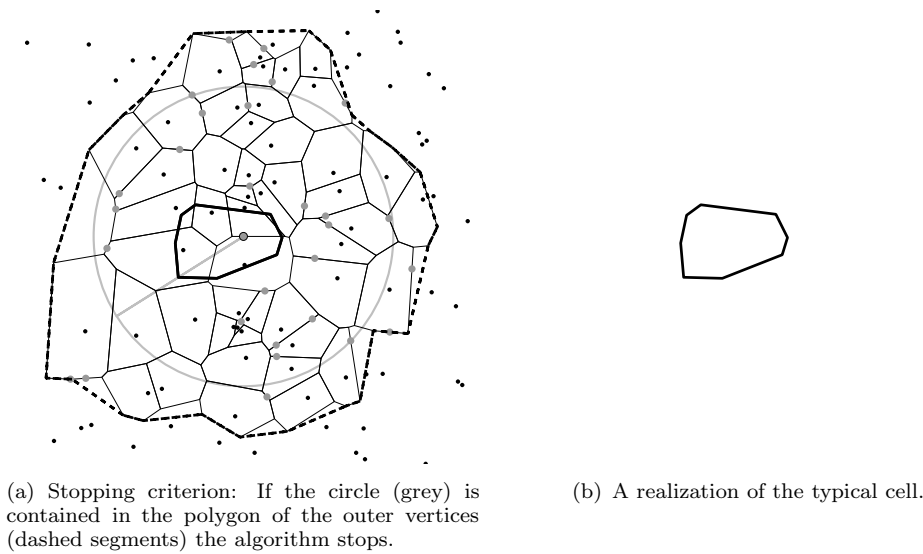(b) A realization of the typical cell.

Figure 4. Stopping criterion and simulated cell for the direct algorithm

([15]) under the condition that $B(o, R) \cap X_p = \emptyset$ until the Voronoi cell Ξ_1 around X_1 with respect to $\widetilde{X}_p = X_{p,R} \cup \{X_1, X_2\}$ can be constructed. Then, simulate points of X_c^* as linear Poisson processes on the edges of Ξ_1 and add $X_{1,c} = o$ to X_c^*. This is done by first simulating the number of points $N \sim \mathrm{Poi}(\lambda_\ell \nu_1(\partial \Xi_1))$ on $\partial \Xi_1$ and then, given $N = n$, by placing n points independently and uniformly distributed on $\partial \Xi_1$. Then new points of $\widetilde{X}_p$ are simulated and cells Ξ_n are constructed. On the new line segments further points of X_c^* are placed as linear Poisson processes. If it is possible, an initial cell is constructed around o from the points of X_c^* simulated so far. In order to check for the possibility of constructing an initial cell a cone criterion can be used, see [4], [15] and [19]. In case that this is not yet possible, further cells of $\widetilde{T}_{X_p}$ are simulated and points from X_c^* are placed on the new edges. If the initial cell is constructed, then we know that only points of X_c^* in $B(o, r_{max})$ with $r_{max} = 2 \max_{i=1,\ldots,n} |v_i|$ can influence the initial cell. Here, $v_i, i = 1 \ldots, n$ are the vertices of the initial cell. Since we know that the points of X_c^* are located on $\widetilde{T}_{X_p}^{(1)}$, we can stop if all edges of $\widetilde{T}_{X_p}$ which can intersect $B(o, r_{max})$ are already constructed. So we use the following stopping criterion. The vertices of $\widetilde{T}_{X_p}$ which are on the boundary of only one constructed cell are connected in clockwise order. If the resulting (not necessarily convex) polygon contains $B(o, r_{max})$, then all edges are constructed and we can stop. This follows from the convexity of the cells and the property of PVT that with probability one three edges meet at one vertex. Of course, if the initial cell is intersected by the bisector between o and the new point X_n the maximal radius r_{max} can be updated in order to reduce runtime. The stopping criterion is illustrated in Figure 4, together with a simulated zero cell of X_c^*.

Except of a missing isotropic rotation around the origin, the resulting cell is then a realization of the typical cell of PVCVT.

3.3. *Neveu's exchange formula and an indirect simulation algorithm*

In this section we derive an alternative, indirect simulation algorithm. With this algorithm it is possible to simulate cells from which all distributional properties of the typical cell of Cox-Voronoi tessellations T_{X_c} can be obtained for Cox processes

X_c concentrated on the edges of a more general class of stationary random tessellations T. It is merely required that the tessellation T^* distributed according to the Palm distribution $\mathbb{P}_T^*$ of T can be simulated. If we consider T to be a PVT this simulation is easily achieved since in this case we only have to construct the Voronoi tessellation generated by a stationary Poisson process with an additional point at the origin. But there are also other stationary point processes where a similar technique could be used. Examples are Voronoi tessellations based on Cox processes concentrated on PLT ([5]), PVCVT (preceding section), PLCVT ([5]), Poisson-Laguerre tessellations ([8]) or on Voronoi tessellations based on Cox processes ([4]) whose random driving measures depend on Boolean models ([11]). In [9] a related technique is used in order to obtain distributional properties of the typical cell of iterated tessellations. There the typical cell is also not simulated directly, but cells are simulated from which the distribution of characteristics of the typical cell can be obtained.

In the following we focus on Cox processes X_c concentrated on the set of edges $T^{(1)}$ of a stationary random tessellation T with linear intensity λ_ℓ, i.e. Cox processes with driving measure $\Lambda_{X_c}(B) = \lambda_\ell \nu_1(B \cap T^{(1)})$, and the corresponding Voronoi tessellation T_{X_c}. The simulation algorithm is based on a representation formula for the typical cell of T_{X_c} which is stated in Theorem 3.5 below. In order to prove this theorem we need the following auxiliary results.

First note that the Cox-Voronoi tessellation T_{X_c} together with the underlying tessellation T can be regarded as a random variable $Y = (T_{X_c}, T)$ in $N_{\mathcal{P}^o}^2$. We then use the notation $T_{X_c} = \{[X_n^{(1)}, \Xi_n^{(1)}]\}_{n \geq 1}$ and $T = \{[X_n^{(2)}, \Xi_n^{(2)}]\}_{n \geq 1}$ and denote the distribution of Y by $\mathbb{P}_Y$. Let $\lambda^{(1)} = \lambda_c$ and $\lambda^{(2)} = \lambda_T$ denote the intensities of T_{X_c} and T, respectively, seen as marked point processes. We define the Palm distributions $\mathbb{P}_Y^{(i)}, i = 1, 2$ on $\mathcal{N}_{\mathcal{P}^o} \otimes \mathcal{N}_{\mathcal{P}^o} \otimes \mathcal{B}(\mathcal{P}^o)$ with respect to the i-th component of Y by

$$\mathbb{P}_Y^{(i)}(A \times G) = \frac{1}{\lambda^{(i)}} \, \mathbb{E}\#\{n : X_n^{(i)} \in [0,1)^2, \Xi_n^{(i)} \in G, t_{X_n^{(i)}} Y \in A\} \qquad (9)$$

for any $A \in \mathcal{N}_{\mathcal{P}^o} \otimes \mathcal{N}_{\mathcal{P}^o}$ and $G \in \mathcal{B}(\mathcal{P}^o)$. Note that for $A \in \mathcal{N}_{\mathcal{P}^o}, G \in \mathcal{B}(\mathcal{P}^o)$ we get

$$\mathbb{P}_Y^{(1)}(A \times N_{\mathcal{P}^o} \times G) = \mathbb{P}_{T_{X_c}}^*(A \times G) \quad \text{and} \quad \mathbb{P}_Y^{(2)}(N_{\mathcal{P}^o} \times A \times G) = \mathbb{P}_T^*(A \times G),$$

where $\mathbb{P}_{T_{X_c}}^*$ and $\mathbb{P}_T^*$ is the ordinary Palm distribution of the random tessellation T_{X_c} and T, respectively.

Now we are interested in the distribution of Y (more precisely of T_{X_c}) under $\mathbb{P}_Y^{(2)}$. Let $Y^* = (T_{\widetilde{X}_c}, T^*)$ denote a vector of random tessellations distributed according to $\mathbb{P}_Y^{(2)}(\cdot \times \mathcal{P}^o)$, where $\widetilde{X}_c$ denotes the point process consisting of the nuclei of Voronoi tessellation $T_{\widetilde{X}_c}$, and T^* is distributed according to $\mathbb{P}_T^*(\cdot \times \mathcal{P}^o)$.

Lemma 3.3: *The point process $\widetilde{X}_c$ is a (non-stationary) Cox process in $\mathbb{R}^2$ with driving measure $\Lambda_{\widetilde{X}_c}(B) = \lambda_\ell \nu_1(B \cap T^{*(1)})$ for $B \in \mathcal{B}(\mathbb{R}^2)$, where $T^{*(1)}$ denotes the edge set of T^*.*

Proof: For any $n \geq 1$, for arbitrary bounded and pairwise disjoint sets $B_1, \ldots, B_n \in \mathcal{B}(\mathbb{R}^2)$ and for any $k_1, \ldots, k_n \in \mathbb{N}$ consider the set

$$A = \{\psi \in N_{\mathcal{P}^o} : \psi(B_1 \times \mathcal{P}^o) = k_1, \ldots, \psi(B_n \times \mathcal{P}^o) = k_n\}.$$

It is sufficient to show that

$$\mathbb{P}_Y^{(2)}(A \times N_{\mathcal{P}^o} \times \mathcal{P}^o) = \mathbb{E}\Big(\prod_{i=1}^n \frac{(\lambda_\ell \nu_1(B_i \cap T^{*(1)}))^{k_i}}{k_i!} \, e^{-\lambda_\ell \nu_1(B_i \cap T^{*(1)})}\Big). \qquad (10)$$

Using the definition of Cox processes we can decompose the expectation in (9), i.e. the integration with respect to $\mathbb{P}_Y$, into an outer integral with respect to $\mathbb{P}_T$ (in order to realize the random driving measure) and, given $T = \tau$, an inner integration with respect to the distribution $\mathbb{P}_{X_c|T=\tau}$ of a Poisson process with intensity measure $\lambda_\ell \nu_1(\,\cdot\, \cap \tau^{(1)})$. Note that we can identify X_c with the Voronoi tessellation T_{X_c}. Then, with the notation $A' = \{\varphi \in N : \varphi(B_1) = k_1, \ldots, \varphi(B_n) = k_n\}$, we get

$$\mathbb{P}_Y^{(2)}(A \times N_{\mathcal{P}^o} \times \mathcal{P}^o)$$

$$= \frac{1}{\lambda^{(2)}} \int_{N_{\mathcal{P}^o}} \int_N \int_{[0,1)^2 \times \mathcal{P}^o} \mathbb{1}_{A'}(t_x \varphi) \, \tau(d(x,\xi)) \, \mathbb{P}_{X_c|T=\tau}(d\varphi) \, \mathbb{P}_T(d\tau)$$

$$= \frac{1}{\lambda^{(2)}} \int_{N_{\mathcal{P}^o}} \int_{[0,1)^2 \times \mathcal{P}^o} \int_N \mathbb{1}_{A'}(t_x \varphi) \, \mathbb{P}_{X_c|T=\tau}(d\varphi) \, \tau(d(x,\xi)) \, \mathbb{P}_T(d\tau)$$

$$= \frac{1}{\lambda^{(2)}} \int_{N_{\mathcal{P}^o}} \int_{[0,1)^2 \times \mathcal{P}^o} \int_N \mathbb{1}_{A'}(\varphi) \, \mathbb{P}_{X_c|T=t_x\tau}(d\varphi) \, \tau(d(x,\xi)) \, \mathbb{P}_T(d\tau)$$

$$= \frac{1}{\lambda^{(2)}} \int_{N_{\mathcal{P}^o}} \int_{[0,1)^2 \times \mathcal{P}^o} \prod_{i=1}^n \frac{(\lambda_\ell \nu_1(B_i \cap (t_x\tau)^{(1)}))^{k_i}}{k_i! \, e^{\lambda_\ell \nu_1(B_i \cap (t_x\tau)^{(1)})}} \, \tau(d(x,\xi)) \, \mathbb{P}_T(d\tau).$$

Now the refined Campbell theorem for stationary marked point processes (see e.g. Satz 3.4.3 of [16]) can be applied to get

$$\mathbb{P}_Y^{(2)}(A \times N_{\mathcal{P}^o} \times \mathcal{P}^o) = \int_{[0,1)^2} \int_{N_{\mathcal{P}^o} \times \mathcal{P}^o} \prod_{i=1}^n \frac{(\lambda_\ell \nu_1(B_i \cap \tau^{(1)}))^{k_i}}{k_i! \, e^{\lambda_\ell \nu_1(B_i \cap \tau^{(1)})}} \, \mathbb{P}_T^*(d(\tau,\xi)) \, dx$$

$$= \mathbb{E}\Big(\prod_{i=1}^n \frac{(\lambda_\ell \nu_1(B_i \cap T^{*(1)}))^{k_i}}{k_i!} \, e^{-\lambda_\ell \nu_1(B_i \cap T^{*(1)})}\Big).$$

Thus, (10) is shown. $\qquad\qquad\qquad\qquad\qquad\qquad\qquad\qquad\qquad\qquad\qquad\square$

Furthermore, in the proof of Theorem 3.5, we utilize Neveu's exchange formula ([13]). This formula allows to represent the expectation of functionals of $Y = (T_{X_c}, T)$ with respect to $\mathbb{P}_Y^{(1)}$ by the expectation with respect to $\mathbb{P}_Y^{(2)}$. Using the notation introduced above, Neveu's exchange formula takes the following form (see e.g. [9]).

Lemma 3.4: *For any measurable function* $f : \mathbb{R}^2 \times \mathcal{P}^o \times \mathcal{P}^o \times N_{\mathcal{P}^o}^2 \to [0,\infty)$, *it holds that*

$$\lambda^{(1)} \int_{N_{\mathcal{P}^o}^2 \times \mathcal{P}^o} \int_{\mathbb{R}^2 \times \mathcal{P}^o} f(x, \xi_1, \xi_2, t_x \psi) \, \psi^{(2)}(d(x,\xi_2)) \, \mathbb{P}_Y^{(1)}(d(\psi, \xi_1))$$

$$= \lambda^{(2)} \int_{N_{\mathcal{P}^o}^2 \times \mathcal{P}^o} \int_{\mathbb{R}^2 \times \mathcal{P}^o} f(-x, \xi_1, \xi_2, \psi) \, \psi^{(1)}(d(x,\xi_1)) \, \mathbb{P}_Y^{(2)}(d(\psi, \xi_2)), \tag{11}$$

where $\psi = (\psi^{(1)}, \psi^{(2)}) \in N_{\mathcal{P}^o}^2$.

Using Lemmas 3.3 and 3.4, we now derive a representation formula which is crucial for the indirect simulation algorithm.

Theorem 3.5:   *Let $h : \mathcal{P}^o \to [0, \infty)$ be a Borel–measurable function, which is translation-invariant, i.e., $h(\xi) = h(\xi + x)$ for any $\xi \in \mathcal{P}^o$ and $x \in \mathbb{R}^2$. Then,*

$$\mathbb{E}\, h(\Xi_c^*) = \frac{1}{\mathbb{E}\, \nu_1(\partial \Xi_T^*)} \, \mathbb{E}\left(\nu_1(\partial \Xi_T^*)\, \mathbb{E}\left(h(\Xi_{\widetilde{X}_c \cup \{Z\}}(Z)) \mid T^*\right)\right), \tag{12}$$

where Ξ_c^* denotes the typical cell of T_{X_c} and Ξ_T^* denotes the zero cell of T^*. Furthermore, $\Xi_{\widetilde{X}_c \cup \{Z\}}(Z)$ denotes the Voronoi cell around an additional point $Z \in \partial \Xi_T^*$ with respect to $\widetilde{X}_c \cup \{Z\}$. This point Z is conditionally uniformly distributed on $\partial \Xi_T^*$ and conditionally independent of $\widetilde{X}_c$ given T^*.

Proof: Consider the function $f : \mathbb{R}^2 \times \mathcal{P}^o \times \mathcal{P}^o \times N_{\mathcal{P}^o}^2 \to [0, \infty)$ given by

$$f(x, \xi_c, \xi, \psi) = \begin{cases} h(\xi_c) & \text{if } o \in \partial \xi + x, \\ 0 & \text{otherwise,} \end{cases} \tag{13}$$

i.e., $f(x, \xi_c, \xi, \psi) = h(\xi_c)$ if the cell $\xi + x$ centred at x contains the origin on its boundary. Then, applying Lemma 3.4, we get that

$$\mathbb{E}\, h(\Xi_c^*) = \int_{N_{\mathcal{P}^o}^2 \times \mathcal{P}^o} h(\xi_c)\, \mathbb{P}_Y^{(1)}(d(\psi, \xi_c))$$

$$= \frac{1}{2} \int_{N_{\mathcal{P}^o}^2 \times \mathcal{P}^o} \int_{\mathbb{R}^2 \times \mathcal{P}^o} f(x, \xi_c, \xi, t_x \psi)\, \psi^{(2)}(d(x, \xi))\, \mathbb{P}_Y^{(1)}(d(\psi, \xi_c))$$

$$= \frac{\lambda^{(2)}}{2\lambda^{(1)}} \int_{N_{\mathcal{P}^o}^2 \times \mathcal{P}^o} \int_{\mathbb{R}^2 \times \mathcal{P}^o} f(-x, \xi_c, \xi, \psi)\, \psi^{(1)}(d(x, \xi_c))\, \mathbb{P}_Y^{(2)}(d(\psi, \xi)).$$

Note that the factor $1/2$ appears due to the fact that for each point of X_c that is located on one (and only one) edge of T, there are exactly two cells of T that have this point of X_c on their boundary. Furthermore, the outer integration in the latter expression can be decomposed into an outer integral with respect to $\mathbb{P}_T^*$ and an inner integral with respect to $\mathbb{P}_{T_{\widetilde{X}_c} | T^*}$. Thus, using the definition of the function f given in (13), we get

$$\mathbb{E}\, h(\Xi_c^*) = \frac{\lambda^{(2)}}{2\lambda^{(1)}} \, \mathbb{E}\left(\mathbb{E}\left(\int_{\partial \Xi_T^* \times \mathcal{P}^o} h(\xi_c)\, T_{\widetilde{X}_c}(d(x, \xi_c)) \mid T^*\right)\right). \tag{14}$$

From Lemma 3.3 we get that the conditional expectation given T^* is the expectation with respect to a PVT induced by a Poisson process which is concentrated on the edges of T^* with linear intensity λ_ℓ. This means in particular that for given T^* the number $S = T_{\widetilde{X}_c}(\partial \Xi_T^* \times \mathcal{P}^o)$ of points on the boundary $\partial \Xi_T^*$ of the zero cell Ξ_T^* of T^* is Poisson distributed with mean $\eta = \lambda_\ell \nu_1(\partial \Xi_T^*)$. It is well known that for given T^* and $S = n$ the locations of these n points can be described by an n-dimensional random vector $(Z_1, \dots, Z_n)$ whose components are independent and (identically) uniformly distributed on $\partial \Xi_T^*$. Moreover, the random vector $(Z_1, \dots, Z_n)$ is conditionally independent of the locations of those points of $\widetilde{X}_c$ which are not located on $\partial \Xi_T^*$.

Let $\Xi_1, \dots, \Xi_n$ denote the Voronoi cells with the nuclei $Z_1, \dots, Z_n$ of the corresponding (conditional) PVT. Note that the cells $\Xi_1, \dots, \Xi_n$ are not independent,

but they are identically distributed. This gives

$$
\mathbb{E}\left(\int_{\partial \Xi_T^* \times \mathcal{P}^o} h(\xi_c)\, T_{\widetilde{X}_c}(d(x,\xi_c)) \mid T^*\right)
$$

$$
= \sum_{n=1}^{\infty} \mathbb{P}(S=n \mid T^*)\, \mathbb{E}\left(\sum_{i=1}^{n} h(\Xi_i) \mid S=n,\, T^*\right)
$$

$$
= \sum_{n=1}^{\infty} \mathbb{P}(S=n \mid T^*)\, n\, \mathbb{E}\left(h(\Xi_1) \mid S=n,\, T^*\right)
$$

$$
= \eta \sum_{n=1}^{\infty} \mathbb{P}(S=n-1 \mid T^*)\, \mathbb{E}\left(h(\Xi_1) \mid S=n,\, T^*\right)
$$

$$
= \eta \sum_{n=0}^{\infty} \mathbb{P}(S=n \mid T^*)\, \mathbb{E}\left(h(\Xi_1) \mid S=n+1,\, T^*\right).
$$

Note that $\mathbb{E}\left(h(\Xi_1) \mid S=n+1,\, T^*\right) = \mathbb{E}\left(h(\Xi_{\widetilde{X}_c \cup \{Z\}}(Z)) \mid S=n,\, T^*\right)$, where the random variable Z is conditionally uniformly distributed on $\partial \Xi_T^*$ and conditionally independent of $\widetilde{X}_c$, given $S=n$ and T^*, and $\Xi_{\widetilde{X}_c \cup \{Z\}}(Z)$ denotes the Voronoi cell around the additional point $Z \in \partial \Xi_T^*$ with respect to $\widetilde{X}_c \cup \{Z\}$. Thus, using (14), we get that

$$
\mathbb{E}\, h(\Xi_c^*) = \frac{\lambda_\ell \lambda^{(2)}}{2\lambda^{(1)}}\, \mathbb{E}\left(\nu_1(\partial \Xi_T^*)\, \mathbb{E}\left(h(\Xi_{\widetilde{X}_c \cup \{Z\}}(Z)) \mid T^*\right)\right).
$$

Since $\lambda^{(1)} = \lambda_\ell \mathbb{E}\nu_1(T^{(1)} \cap [0,1]^2)$ and $\mathbb{E}\nu_1(\partial \Xi_T^*) = 2/\lambda^{(2)}\mathbb{E}\nu_1(T^{(1)} \cap [0,1]^2)$, this completes the proof. $\qquad\square$

Now we summarize the indirect simulation algorithm for the typical cell of PVCVT which is justified by Theorem 3.5. Thus, from now on, we assume that $T = T_{X_p}$, where X_p is a stationary Poisson process with intensity λ_p and Ξ_p^* is the typical cell of T_{X_p}. Note that then $\mathbb{E}\nu_1(\partial \Xi_p^*) = 4/\sqrt{\lambda_p}$.

   1. Simulate a Poisson process $X_p = \{X_i\}_{i \geq 1}$ radially with intensity λ_p, add the origin to X_p, which gives $X_p^* = X_p \cup \{o\}$.
   2. Construct the Voronoi cell Ξ_p^* of $T_{X_p^*}$ around o.
   3. Place independently and uniformly distributed the points $\{Z_i\}_{1 \leq i \leq n}$ of $\widetilde{X}_c$ on the boundary of Ξ_p^*. Here n is the realization of a random variable $S \sim \text{Poi}(\lambda_\ell \nu_1(\partial \Xi_p^*))$. Place one additional point Z independently of the other points and uniformly on $\partial \Xi_p^*$.
   4. Construct further edges of $T_{X_p}^*$ and place points $X_{i,c}$ of $\widetilde{X}_c$ on the edges according to linear Poisson processes.
   5. Construct the Voronoi cell $\Xi_{\widetilde{X}_c \cup \{Z\}}$ around Z.
   6. Weight $h(\Xi_{\widetilde{X}_c \cup \{Z\}})$ by $\nu_1(\partial \Xi_p^*)\sqrt{\lambda_p}/4$.

Then, with the weighted value $\sqrt{\lambda_p}/4\, \nu_1(\partial \Xi_p^*)\, h(\Xi_{\widetilde{X}_c \cup \{Z\}})$ we can obtain the distribution of $h(\Xi_c^*)$. An overview of the different steps is shown in Figure 5. Note that indirect simulation algorithm is similar to the direct simulation algorithm, but now we have to construct a cell around Z, so we have to adjust the stopping criterion of the direct algorithm by choosing the maximal radius as $r_{max} = \max_{i=1,\dots,n}(|v_i| + |v_i - Z|)$. Again $v_i, i = 1,\dots,n$ denote the ver-

(a) Start: The cell around the origin is constructed, points (grey) of $\widetilde{X}_c$ are placed on the boundary and one further point Z (grey with black boundary) is added.

(b) Initial cell: The initial cell around Z is constructed using the previously simulated points (grey) of $\widetilde{X}_c \cup \{Z\}$.

(c) Further points of $\widetilde{X}_c$ are simulated (grey) and the initial cell is intersected by the bisectors.

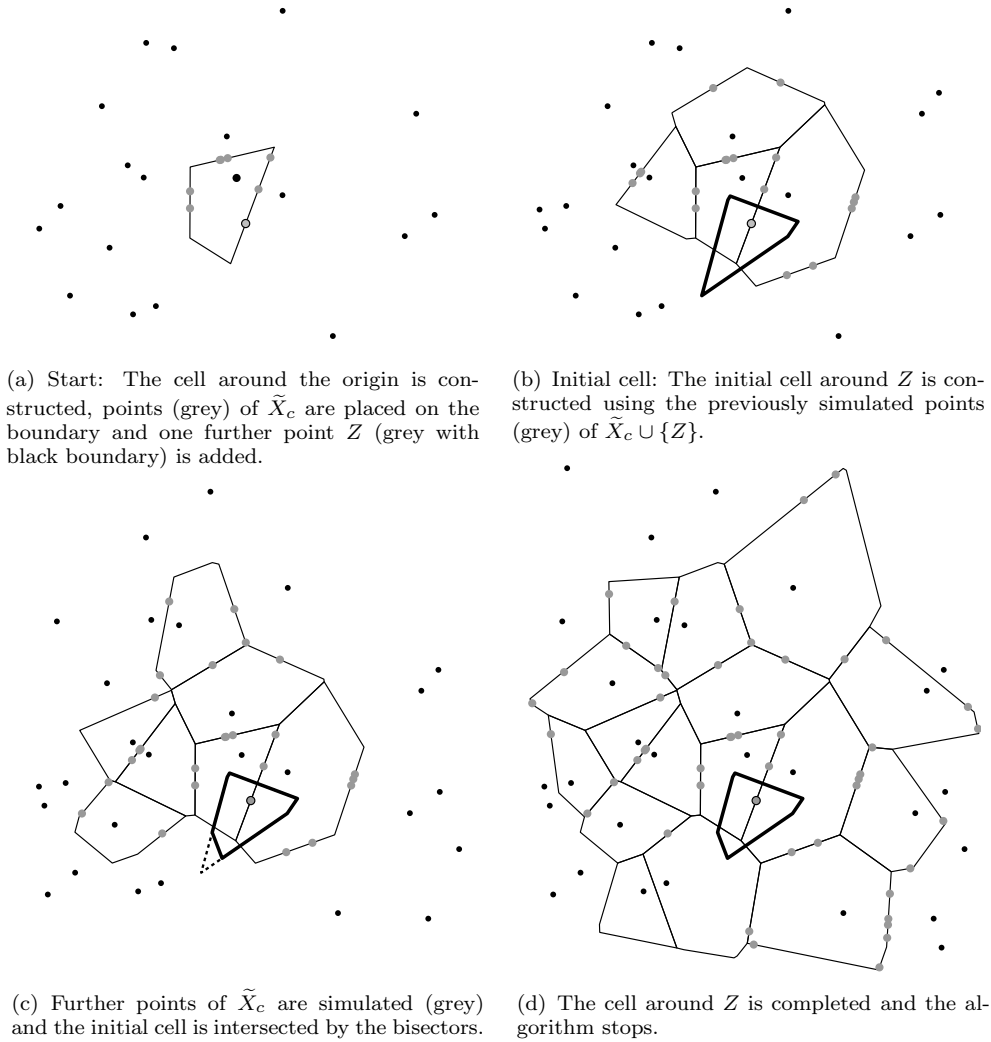(d) The cell around Z is completed and the algorithm stops.

Figure 5. Indirect simulation of the typical PVCV cell

tices of the initial cell, see Figure 6. The result of the simulation algorithm is then a cell $\Xi_{\widetilde{X}_c \cup \{Z\}}$. This cell can be used to estimate characteristics of the typical cell Ξ_c^*. For given $T_{X_p}^*$ with typical cell Ξ_p^* consider the random variable $h_Z = \nu_1(\partial \Xi_p^*) h(\Xi_{\widetilde{X}_c \cup \{Z\}})$. If we then regard independent copies $h_{Z,1}, ..., h_{Z,n}$ of h_Z we can define the estimator $\widehat{h}$ by

$$\widehat{h} = \frac{\sqrt{\lambda_p}}{4} \frac{1}{n} \sum_{i=1}^{n} h_{Z,i}. \tag{15}$$

Then $\widehat{h}$ is unbiased for $\mathbb{E}\, h(\Xi_c^*)$ due to Theorem 3.5.

(a) Stopping criterion: If the circle (grey) is contained in the polygon of the outer vertices (dashed segments) the algorithm stops.

(b) Simulated cell (black) with typical cell (grey) of the PVT used for the weighting
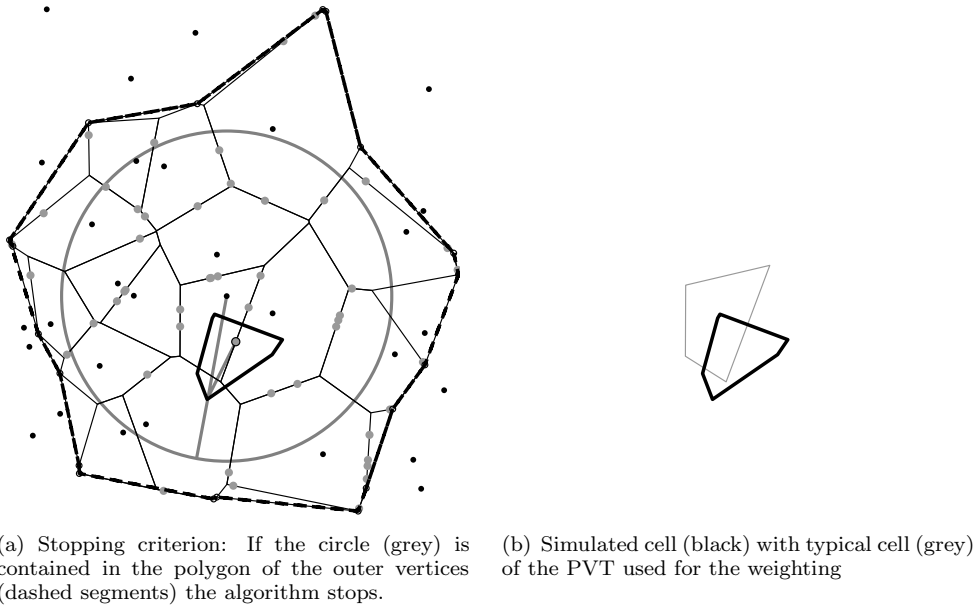
Figure 6. Stopping criterion and simulated cell for the indirect algorithm

4.   Numerical results

4.1.   *Scaling invariance*

Recall that the Poisson-Voronoi-Cox process X_c and the PVCVT T_{X_c} can be fully characterized by two parameters: λ_ℓ and λ_p. But a scaling invariance can be observed which means that the structural properties of X_c and T_{X_c} do not change if the x–axis and the y–axis are scaled in the same way. This implies that with respect to numerical computations it suffices to regard a one-dimensional parameter space with a single parameter κ, i.e., instead of the originally two-dimensional parameter $(\lambda_\ell, \lambda_p)$ consider the *scaling factor* $\kappa = 2\sqrt{\lambda_p}/\lambda_\ell$, which is the mean total length of edges of T_{X_p} per unit area divided by the mean number of points of X_c per unit length of T_{X_p}. If the x–axis and the y–axis are scaled in the same way, then κ remains constant, and hence the same random structure is obtained, but on different scales. For example, for different parameter pairs $(\lambda_\ell, \lambda_p)$ and $(\lambda'_\ell, \lambda'_p)$ with $(\lambda'_\ell, \sqrt{\lambda'_p}) = a\,(\lambda_\ell, \sqrt{\lambda_p})$ for some $a > 0$, we get $\mathbb{E}\nu_0(\Xi_c^{*\prime}) = \mathbb{E}\nu_0(\Xi_c^*)$, $\mathbb{E}\nu_1(\partial\Xi_c^{*\prime}) = a\mathbb{E}\nu_1(\partial\Xi_c^*)$ and $\mathbb{E}\nu_2(\Xi_c^{*\prime}) = a^2\mathbb{E}\nu_2(\Xi_c^*)$ where Ξ_c^* and $\Xi_c^{*\prime}$ denote the typical cells of the PVCVT corresponding to the parameter pairs $(\lambda_\ell, \lambda_p)$ and $(\lambda'_\ell, \lambda'_p)$, respectively, and $\nu_0(\Xi)$ denotes the number of vertices of a cell Ξ. On the other hand, for large κ we only get a few points per edge of the PVT T_p, whereas for small values of κ we get many points per edge.

In [5] and [6] a similar effect for PLCVT is used to reduce the number of parameters in the numerical experiments. Namely, using scaling invariance, it is sufficient to do computations for each κ only for one parameter pair (λ_l, λ_p). For all other parameter pairs with the same scaling factor κ these numerical results can then be used to calculate, for example, estimated mean values of different characteristics by appropriate scaling. In addition the outputs of simulations with different parameter pairs but equal κ can be used for implementation tests, see Section 4.2.

For $\kappa \in \{10, 20, 30, 40, 50, 60, 90, 120\}$ and $2\sqrt{\lambda_p} = 1$ we simulated in each case 1 000 000 cells with both algorithms which are used in the following.

4.2. *Implementation Tests*

First, we used the simulated cells to test the correctness of the implementation of
the algorithms, where methods for software tests with random output are suitable
([5],[10]). In particular, we compared the output of the implementations of the two
introduced algorithms in order to test the correctness of the implementation. This
test can be performed in a similar way as the software tests proposed in [5], i.e.,
an asymptotic Gaussian two sample test for equal means is performed to compare
characteristics like the mean perimeter, area or number of vertices of the outputs
of the two algorithms for different parameters. All the tests showed the expected
behaviour, so we assume that our implementations are correct.

4.3. *Comparison of the direct and indirect algorithm*

The sample means of cell characteristics for the directly simulated cells and the
sample means of the weighted characteristics for the cells of the indirect algorithm
should be equal, but the variances might differ since we are considering different
random variables. So we computed the sample variances of the (weighted) number
of vertices (ν_0), perimeter (ν_1) and area (ν_2) of the simulated cells for both algo-
rithms. The results are displayed in Table 1 for different values of κ. It can be seen
that the variance of the output of the direct algorithm is always smaller. Since
both algorithms have similar runtimes, the variance of the (random) output is the
main criterion which algorithm is preferable for the computation of distributional
properties. Because of that we concentrate in the following only on results for the
directly simulated cells, although the indirect algorithm yields similar results.

Note that especially for the computation of shortest path lengths ([7]) it is im-
portant to have an algorithm with low variance of the output, since due to time-
consuming computations only a relatively small sample size can be considered.
Thus, also for this purpose, the direct algorithm should be preferred.

4.4. *Comparison of distributional properties of PVT, PLCVT and PVCVT*

The simulated cells have been used to compute histograms for the area, perime-
ter and number of vertices of the typical cell of PVCVT as well as the coefficient
of variation ($\mathrm{cv}X := \sqrt{\mathrm{Var}X}/\mathbb{E}X$) of these characteristics. Furthermore, we esti-
mated the mean boundary length of the typical cell. The results are displayed in
Figure 7 and in Tables 2 and 3, respectively, together with corresponding results
for the typical cell of PLCVT ([5]) and PVT. The parameters for PVT, PVCVT
and PLCVT were chosen such that the expected area of the typical cell is equal to
100 and, for PVCVT and PLCVT, the scaling factor κ is the same, i.e., the mean
edge lengths per unit area of the underlying PVT and PLT, respectively, are equal.

Although the shapes of the histograms in Figure 7 seem to be similar, we can ob-
serve a large difference between the histograms for PLCVT and PVCVT, especially
for small values of κ. This difference seems to decrease with increasing κ, but also
for large values of κ it is still noticeable. Similar effects can be observed in Tables 2
and 3. For PVCVT the cv is decreasing with increasing κ for all characteristics,
but it is always smaller than the cv of the same characteristics for PLCVT. As
mentioned above, the mean area is 100 and the mean number of vertices is 6 for
all values of κ, but the mean boundary length depends on the scaling factor κ,
see Table 3. For PVCVT the estimated mean boundary length only slightly differs
from 40, the expected boundary length for PVT, and statistical significance tests
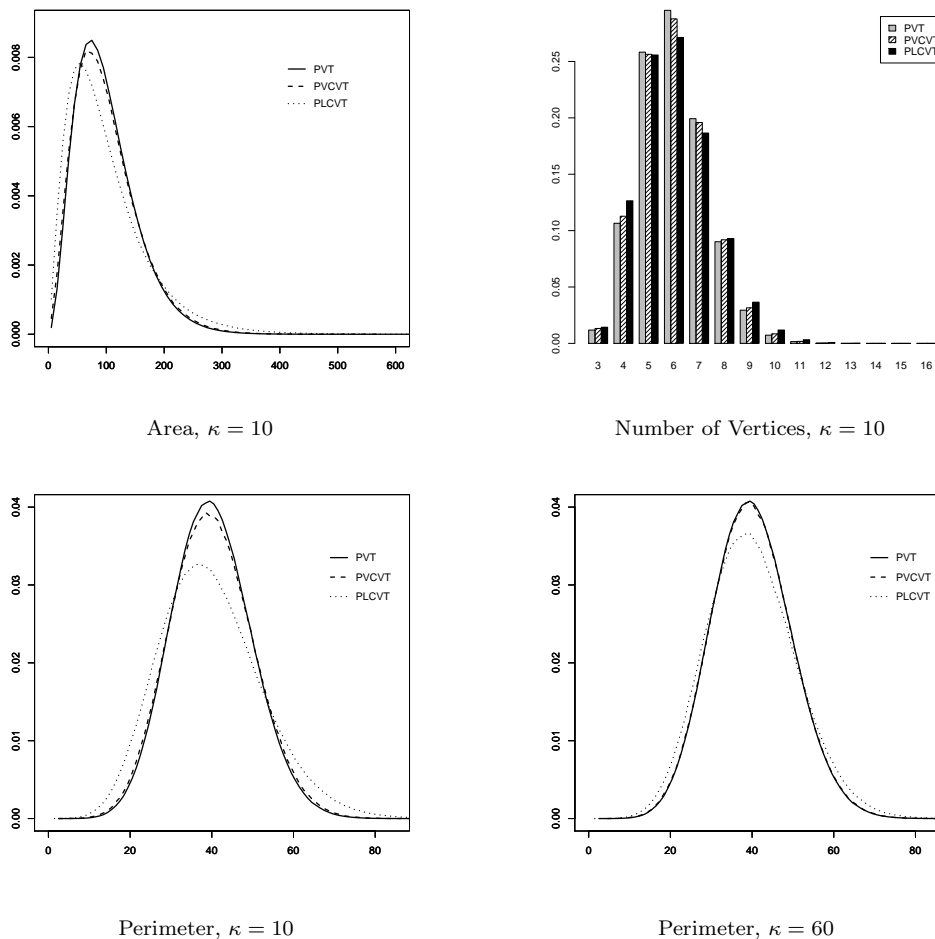for equality do not lead to rejection. However, for PLCVT the estimated boundary

Figure 7. Histograms for characteristics of the typical cell

length is always significantly smaller than 40.

These differences might be caused by the larger irregularity of PLT compared to PVT. If the expected edge lengths per unit area of both tessellations are equal, then the segments of PVT are more evenly spread in the plane and the variations within these segments is much smaller than for PLT. Furthermore, infinitely many nuclei are located on each single line of PLCVT with probability 1, whereas this is not possible for PVCVT.

Comparing PVCVT to PVT, the shapes of the histograms in Figure 7 are quite similar, but there is some difference which is decreasing with κ. From Tables 2 and 3 we can see that for PVCVT the cv of the considered characteristics is always slightly larger than for PVT and decreasing with κ. But this difference is much smaller than the difference to PLCVT and seems to become negligible for large values of κ.

Altogether there seems to be a quite large difference between the distributions of cell characteristics of PLCVT and PVCVT, especially for small values of κ. This difference is decreasing with increasing κ, but seems to be noticeable also for large values of κ. On the other hand, the distributions of cell characteristics of PVCVT and PVT seem to be similar and for large values of κ almost identical. However, note that for the estimation of shortest path lengths in telecommunication network models the typical cell has to be simulated together with the underlying tessellation. Thus, also for large values of κ, the PVCVT is still an interesting model.

5.   Discussion and Outlook

We presented two different algorithms for the simulation of the typical cell of
PVCVT, where we compared these algorithms with respect to precision and run-
time. The direct algorithm is preferable from this point of view since the runtimes
are almost equal, but the variance in the random output of the direct algorithm
is smaller. Nevertheless the indirect algorithm has some advantages, too. First, it
can be used for implementation tests. On the other hand, it is more general and
can be used for a variety of Cox-Voronoi tessellations, whereas the direct algorithm
can only be used in the special case of PVCVT, because it seems to be very difficult
and perhaps impossible to get a similar Palm representation as in Lemma 3.2 for
other models than PVT.

The numerical results show that the typical cell of PVCVT is much more sim-
ilar to the typical cell of ordinary PVT than to the typical cell of PLCVT. This
observation can probably be explained by the fact that especially for large values
of κ the likelihood of three or more points of the PVCV process to be located on
the same edge of the underlying Voronoi tessellation is close to zero. Therefore,
the dependence between different points of the PVCV process almost vanishes for
larger κ. This leads to a point process that behaves quite similar to a Poisson
point process, in particular with regard to the induced Voronoi tessellation. For a
PLCVT these arguments do not hold to such an extend due to the fact that even
for very large κ we find infinitely many points of the PLCV point process to be
located on a specific line of the underlying Poisson line process.

Simulation algorithms for the typical cell of PVCVT are a useful tool in order to
perform cost analysis in telecommunication networks. Together with the techniques
described in [7], the computation of shortest path lengths and similar characteristics
can be extended to new models. So far only PLT have been considered as models
for the roads, but by using the results of the present paper also PVT can be taken
into account.

A further step in the development of an adequate pool of possible tessellation
models for the cost analysis of telecommunication networks is the extension of the
methods described here to simulation algorithms for the typical cell of models like
the Poisson-Delaunay tessellation (PDT) and iterated tessellations. Together with
efficient techniques for the simulation of shortest paths and the computation of
their length, such algorithms will lead to a portfolio of realistic cost models that
can be fitted to given telecommunication data, in order to enable cost calculation
and, sometimes even more important, cost prediction.

Acknowledgements

References

[1] V. Baumstark and G. Last. Some distributional results for Poisson Voronoi tessellations. *Advances
     in Applied Probability*, 39:16–40, 2007.
[2] B. Błaszczyszyn and R. Schott. Approximations of functionals of some modulated Poisson–Voronoi

	Direct Algorithm			Indirect Algorithm		
κ	ν_1	ν_2	ν_0	ν_1	ν_2	ν_0
10	652.75	124680.35	1.87	1497.86	175659.46	4.36
20	1266.92	479859.33	1.82	2812.88	653731.80	4.26
30	1874.68	1065937.19	1.81	4086.39	1426403.79	4.22
40	2484.18	1881871.79	1.81	5354.02	2492851.63	4.17
50	3098.75	2931215.45	1.80	6624.04	3855095.79	4.17
60	3689.98	4194702.08	1.79	7882.49	5510771.23	4.15
90	5511.02	9384330.87	1.79	11644.29	12187366.14	4.11
120	7336.33	16670645.20	1.79	15406.61	21481790.15	4.10

Table 1.   Sample variances for perimeter (ν_1), area (ν_2) and number of vertices (ν_0) of the typical cell obtained for the direct (left) and indirect (right) simulation algorithm, respectively, where $2\sqrt{\lambda_p} = 0.125$ is fixed.

	cv ν_0			cv ν_2		
κ	PVCVT	PLCVT	PVT	PVCVT	PLCVT	PVT
10	22.784	24.091	22.240	55.174	69.538	52.947
20	22.496	23.454	22.240	54.085	64.819	52.947
30	22.431	23.200	22.240	53.733	62.638	52.947
40	22.386	23.056	22.240	53.564	61.340	52.947
50	22.378	22.929	22.240	53.544	60.516	52.947
60	22.324	22.870	22.240	53.342	59.792	52.947
90	22.292	22.752	22.240	53.203	58.595	52.947
120	22.303	22.669	22.240	53.173	57.836	52.947

Table 2.   Estimates for the cv of the number of vertices (ν_0) and area (ν_2) of the typical cell for PVCVT, PLCVT and PVT and for different values of κ, using the direct algorithm

	PVCVT		PLCVT		PVT	
κ	$\mathbb{E}\nu_1$	cvν_1	$\mathbb{E}\nu_1$	cvν_1	$\mathbb{E}\nu_1$ (exact)	cvν_1
10	40.010	25.242	39.726	31.469	40.0	24.315
20	40.005	24.869	39.766	29.580	40.0	24.315
30	40.008	24.698	39.791	28.684	40.0	24.315
40	40.010	24.621	39.810	28.130	40.0	24.315
50	39.982	24.613	39.812	27.776	40.0	24.315
60	39.997	24.508	39.834	27.474	40.0	24.315
90	39.992	24.458	39.849	26.944	40.0	24.315
120	39.994	24.438	39.884	26.590	40.0	24.315

Table 3.   Estimates for expectation and cv of the boundary length $\nu_1(\partial\Xi^*)$ of the typical cell for PVCVT, PLCVT and PVT and for different values of κ, using the direct algorithm (where $\mathbb{E}\nu_2(\Xi^*) = 100$ is fixed)

tessellations with applications to modeling of communication networks. *Advances in Applied Probability*, 22(2):179–204, 2005.
[3] F. Fleischer. *Analysis and Fitting of Random Tessellation Models. Applications in Telecommunication and Cell Biology.* PhD thesis, Universität Ulm, 2007, http://vts.uni-ulm.de/docs/2007/5941/vts_5941_7959.pdf.
[4] F. Fleischer, C. Gloaguen, H. Schmidt, V. Schmidt, and F. Schweiggert. Simulation of typical modulated Poisson-Voronoi cells and their application to telecommunication network modelling *Japan Journal of Industrial and Applied Mathematics* (under Revision), 2008.
[5] C. Gloaguen, F. Fleischer, H. Schmidt, and V. Schmidt. Simulation of typical Cox-Voronoi cells, with a special regard to implementation tests. *Mathematical Methods of Operations Research*, 62:357–373, 2005.
[6] C. Gloaguen, F. Fleischer, H. Schmidt, and V. Schmidt. Fitting of stochastic telecommunication network models, via distance measures and Monte-Carlo tests. *Telecommunication Systems*, 31:353–377, 2006.

[7] C. Gloaguen, F. Fleischer, H. Schmidt, and V. Schmidt. Analysis of shortest paths and subscriber line lengths in telecommunication access networks. *Networks and Spatial Economics* (to appear), 2008.

[8] C. Lautensack. *Random Laguerre Tessellations*. PhD thesis, Universität Karlsruhe (TH), 2007.

[9] R. Maier, J. Mayer, and V. Schmidt. Distributional properties of the typical cell of stationary iterated tessellations. *Mathematical Methods of Operations Research*, 59:287–302, 2004.

[10] J. Mayer and R. Guderlei. Test oracles of randomness. *Lecture Notes in Informaticcs*, P-58:179–189, 2004.

[11] I.S. Molchanov. *Statistics of the Boolean Models for Practitioners and Mathematicians*. J. Wiley & Sons, Chichester, 1996.

[12] I.S. Molchanov. *Theory of Random Sets*. Springer, London, 2005.

[13] J. Neveu. Sur les mesures de palm de deux processus ponctuels stationnaires. *Zeitschrift für Wahrscheinlichkeitstheorie und verwandte Gebiete*, 34:199–203, 1976.

[14] A. Okabe, B. Boots, K. Sugihara, and S. N. Chiu. *Spatial Tessellations*. J. Wiley & Sons, Chichester, second edition, 2000.

[15] M. P. Quine and D. F. Watson. Radial generation of n-dimensional Poisson processes. *Journal of Applied Probability*, 21:548–557, 1984.

[16] R. Schneider and W. Weil. *Stochastische Geometrie*. Teubner, Stuttgart, 2000.

[17] G. J. Schütz, M. Axmann, S. Freudenthaler, H. Schindler, K. Kandror, J. C. Roder, and A. Jeromin. Visualization of vesicle transport along and between distinct pathways in neurites of living cells. *Microscopy Research and Technique*, 63:159–167, 2004.

[18] D. Stoyan, W. S. Kendall, and J. Mecke. *Stochastic Geometry and its Applications*. J. Wiley & Sons, Chichester, second edition, 1995.

[19] J. G. Wendel. A problem in geometric probability. *Mathematica Scandinavica*, 11:109–111, 1962.